INDIAN JOURNAL OF SCIENCE AND TECHNOLOGY

RESEARCH ARTICLE

A Comparative Analysis of Random Forest and Support Vector Machines for Classifying Irrigated Cropping Areas in The Upper-Comoé Basin, Burkina Faso

Farid Traoré[1]*, Sié Palé[2], Aïda Zaré[2], Moussa Karamoko Traoré[1], Blaise Ouédraogo[1], Joachim Bonkoungou[1]

1 Institut de l'Environnement et de Recherches Agricoles, 04 BP 8645 Ouagadougou 04, Burkina Faso
2 Université de Dédougou/Institut des Sciences de l'Environnement et du Développement Rural, BP 176 Dédougou, Burkina Faso

OPEN ACCESS

Received: 10-01-2024
Accepted: 08-02-2024
Published: 14-02-2024

Citation: Traoré F, Palé S, Zaré A, Traoré MK, Ouédraogo B, Bonkoungou J (2024) A Comparative Analysis of Random Forest and Support Vector Machines for Classifying Irrigated Cropping Areas in The Upper-Comoé Basin, Burkina Faso . Indian Journal of Science and Technology 17(8): 713-722. https://doi.org/10.17485/IJST/v17i8.78

* **Corresponding author**.

farid.traore@yahoo.fr

Funding: None

Competing Interests: None

Published By Indian Society for Education and Environment (iSee)

ISSN
Print: 0974-6846
Electronic: 0974-5645

Abstract

Objectives: This study investigates the performance of two machine-learning algorithms in classifying land areas across the Upper-Comoé basin in Burkina Faso. **Methods:** Within the Google Earth Engine data processing environment, Support Vector Machine (SVM) and the Random Forest (RF) algorithms were applied to a Landsat-8 OLI image of March 2019, to discriminate agricultural land areas, with an emphasis on irrigated areas. **Findings:** The results indicated good to excellent classification performance, with overall accuracies and Kappa coefficients between 71% and 99%, and 0.66 and 0.99, respectively. The RF method outperformed the SVM in terms of mapping "accuracy", but in terms of spatial distribution of classes, the SVM method provided a mapping close to reality, due to the density of the classes generated. **Novelty:** Our findings suggest that remote sensing can constitute a tool fully adapted to the needs of services in charge of agricultural water management in Burkina Faso.

Keywords: Irrigation; Random Forest; Support Vector Machine; Google Earth Engine; Burkina Faso

1 Introduction

The sustainable management of natural resources has become challenging given the rapid world population growth and the changing climate patterns worldwide[(1)].The demographic growth recorded in various parts of the world is most often accompanied by an increased use or destruction of natural resources[(2)].Across the Sahelian zone of Africa, drought events occurred frequently due to the extreme variability in rainfall patterns and temperature conditions. Such drought events most often resulted in severe environmental impacts such as the reduction of vegetation cover, land degradation and loss of biodiversity, as well as harsh socio-economic conditions[(3)].Burkina Faso is a country in the Sahel, whose agricultural development is considerably limited by the availability of water in the major agricultural areas[(4)].Agriculture in Burkina Faso is typically rainfed; the vast majority of farmers (97.6%) use rain as a source of water, and

only 2.2% of them use irrigation [5].To cope with the adverse impacts of rainfall variability, the governmental agencies have been committed to an intensification of irrigated agriculture since the 2000s through multiple incentives [6].This has led to a substantial expansion of irrigated areas in certain regions of the country over the years, with greater profits compared to rainfed agriculture [7].However, this expansion of irrigated agricultural areas, most often near water points such as rivers or water reservoirs, has put a noticeable pressure on these water resources. Monitoring irrigation water relies on a good knowledge of the irrigated areas and available water resources. The mapping of irrigated agricultural areas, combined with a study of water needs, enables an improved management of agricultural water [8].Remote sensing-based approaches for mapping irrigated agricultural areas are cost-effective and are particularly useful in low-income countries where resources are limited for field surveys. [9–11] The exploitation of remote sensing images can be done in several ways, ranging from photo-interpretation to classification. Image classification is the process of categorizing and labeling groups of pixels within an image based on user-defined rules [12]. However, finding the right classification algorithm or the right rule(s) can be challenging since the definition and characterization of the entities to be discriminated is not straightforward. A good classification requires the definition of classes whose pixels are more or less homogeneous. For small or fragmented crop areas such as those found in Burkina Faso, this condition is difficult to meet. The size of the crop areas is most often less than that of the satellite image pixel. Moreover, the choice of the classification algorithm can also be challenging. Supervised and unsupervised classification methods were developed in the early 1970s [13].They have been used for decades for classifying remote sensing images. They are pixel-based classification methods solely based on spectral information (i.e., digital number values) [14]. While supervised methods offer a certain comfort to the user who has complete freedom to define their classes and classification parameters, in unsupervised methods the analyst specifies the desired number of classes, and then the computer automatically groups pixels that are statistically similar into categories using clustering algorithms [14]. Among the supervised methods, the maximum likelihood, support vector machine (SVM), random forest (RF), and neural networks algorithms are increasingly being used for land cover and land use classification based on remote sensing data [15].

The objective of this study was to provide a comparative analysis of two supervised classification algorithms for mapping irrigated agricultural areas across the southwest region of Burkina Faso.

2 Methodology

2.1 Study area

The study area is located in the Upper-Comoé, which is a sub-basin of the Comoé River watershed. The average annual rainfall at the Bérégadougou station during 1971-2011 was 1032 mm [16]. The dry and rainy seasons span October to May and June to September, respectively. Rainfall is highly variable from one year to the next, with a decreasing trend in annual totals and number of rainy days observed during 1971-2011. Multiple water courses cross the study area, with the majority being temporary (i.e., linked to the rainy season). Only the Comoé remains year long. Three water reservoirs (Moussodougou, Lobi and Toussiana) are built on the Comoé River and its tributaries Yannon and Lobi. These reservoirs are the main source of water for domestic, industrial and agricultural needs (Figure 1). The main city of the Upper-Comoé basin is Banfora, with 117,000 inhabitants [17].

This region is highly suitable for agriculture, which employs about 63% of the population of Burkina Faso [17]. Surface water intended for dry season agriculture does not always meet the needs of all the applicants in the rice-growing area of Karfiguela, in the sugar-cane complex of Comoé and among the market gardeners installed along the riverbanks. [1,18]

2.2 Overview of the method

The classification method used in this study is based on pixel information. In order to reduce bias, the classifications were carried out on the same images and with the same training areas within a single software environment. A schematic flowchart of the method is presented in Figure 2.

The software environment used is Google Earth Engine (GEE). GEE is a cloud platform providing parallel computing and data catalog services for global geospatial analysis. The calculations are automatically parallelized. The public datasets are in a ready-to-use format and come from the archives of multiple providers including the United States Geological Survey (USGS), the European Space Agency (ESA). GEE provides various built-in methods that help in image preprocessing [13].

In Burkina Faso, irrigated agriculture is practiced intensively between the months of November and April, when surface or groundwater resources are easily accessible. As part of this study, we chose images from the month of March, which enables identification of irrigated agricultural areas. This choice is justified by the fact that during this period most of the natural herbaceous and/or shrubby vegetation are either dried out or in poor condition, though certain types of herbaceous vegetation still persist during this period.

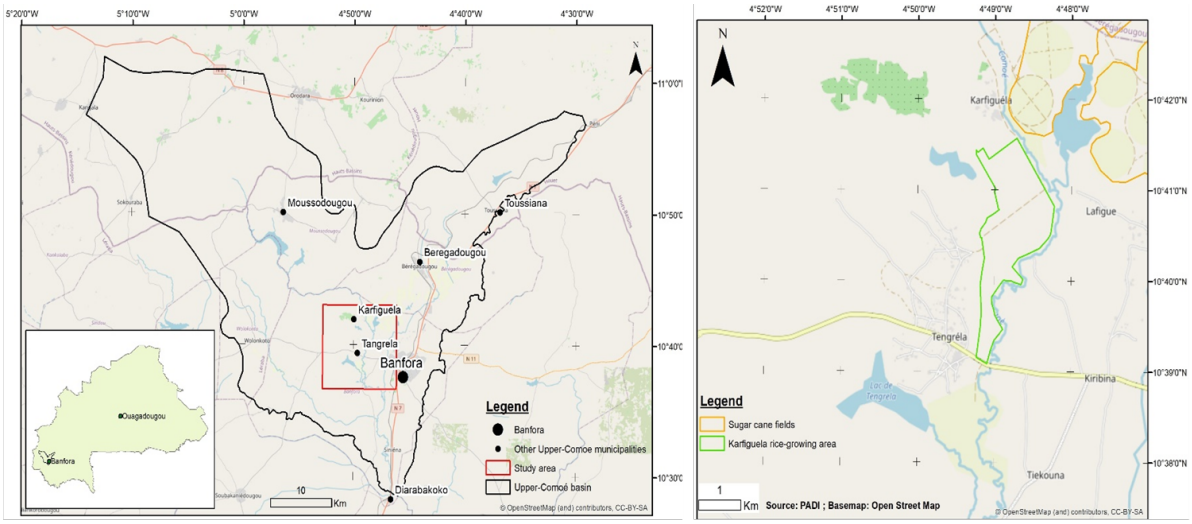

Fig 1. A: Map of the location of the Upper-Comoé watershed and the study area; B: Focus on the study area (Base map: Open Street Map 2024)

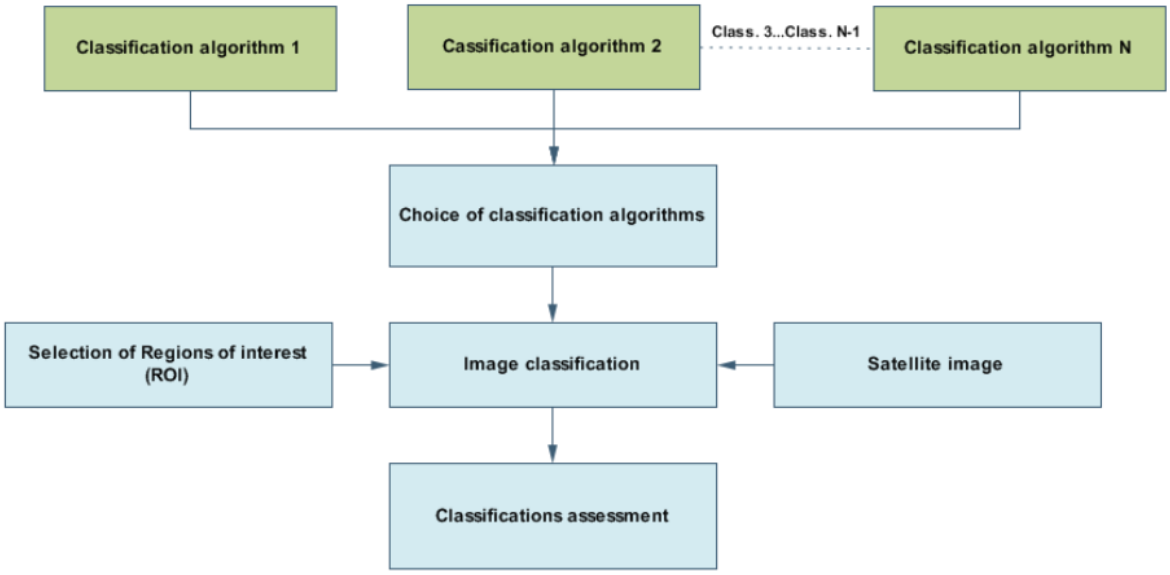

Fig 2. Methodology outline

2.3 Choice of classification methods

Pixel classification algorithms can be grouped into two categories: parametric and non-parametric classifiers. Parametric classifiers assume that the data are representative and normally distributed. Although parametric classifiers such as maximum likelihood have proven to be useful, these classifiers have the major disadvantage of requiring a normal distribution of the land cover data used to train the classifier. However, land cover data generally does not follow a normal distribution.[4,13] On the other hand, non-parametric classifiers such as SVM, RF and artificial neural network (ANN) have proven useful because they do not base the classification on an assumption of normality or on statistical parameters[19]. In our study, we chose the SVM and RF algorithms to classify agricultural land areas in the study zone.

SVM is a classification system derived from statistical learning theory. It separates classes with a decision surface that maximizes the margin between classes. The surface is often called the optimal hyperplane and the data points closest to the hyperplane are called support vectors. The SVM classification method is a non-parametric statistical learning technique.[20–22] It separates classes with a decision surface that maximizes the margin between classes. The surface is often called the optimal hyperplane and the data points closest to the hyperplane are called support vectors. SVMs have gained importance because they are robust and can handle relatively small datasets.[22,23] According to Hsu[24], SVMs include a penalty parameter that allows for a certain degree of misclassification, which is particularly important for non-separable training sets. The penalty parameter controls the trade-off between allowing training errors and forcing rigid margins. This creates a soft margin that allows for some misclassifications, for example allowing some training points on the wrong side of the hyperplane. Increasing the value of the penalty parameter increases the cost C of misclassifying points and forces the creation of a more precise model which may not generalize well[25]. In order to perform an SVM classification, the user must choose a kernel. Various kernel functions exist, such as polynomial kernel, linear kernel, sigmoid kernel, and radial basis kernel or function (RBF). The choice of kernels also affects the classification results. Kernels such as RBF have a user-defined parameter γ that controls the influence of a training sample on the decision boundary. The higher the value of γ, the more tightly fitted the decision boundaries around the samples. Nevertheless, this can lead to overfitting. Therefore, it is necessary to find the right balance[25]. Below are the mathematical representations of sigmoid and radial basis kernels:[26]

RBF: $K(x_i, x_j) = exp(-\gamma \|x_i - x_j\|^2),\ \gamma > 0$

Sigmoid: $K(x_i, x_j) = tan(\gamma x_i^T x_j + r)$

where:

γ *i*s the gamma term in the kernel function for all kernel types except linear.

r is the bias term in the kernel function for the sigmoid kernel.

Random Forest (RF) constructs a set of binary decision trees[27]. Tumer and Ghosh[28] noted that combining the output of multiple classifiers to predict an outcome yields very high classification accuracies. This is the basis of the RF ensemble classifier, which combines the outputs of multiple decision trees to decide the label of a new input data based on a maximum vote. In the context of land use mapping, the number of works using RF continues to increase.[19,29–31] In addition to its comparable performance with other classification algorithms[32],the RF has numerous advantages: reduced calculation time due to the possibility of building the trees in parallel[33], the possibility of taking large volumes of data as input (i.e. a high number of variables), and easier interpretation offered by the visualization of trees. In our study, the sigmoid and radial basis functions were used for the SVM algorithm. Three numbers of forests (10, 50, and 100) were used for the RF algorithm. The classification methods selected will be applied to the same study area, using the same samples of training areas.

2.4 Selection of training areas

Training areas were sampled on the image according to the different land use and land cover (LULC) classes. The selection of training areas was made following field campaigns and supplemented by photo-interpretation using Google Earth. Auxiliary data such as responses to a questionnaire on land and water use administered to a focus group of about 50 institutions (composed, among others, of farmers, agricultural officers, municipal workers, members of the Upper-Comoé basin local water committee, resource people who are long-time residents of the study area), were also used. The LULC selected and number of pixels sampled for each of the classes are presented in Table 1.

Table 1. LULC classes

Classes	Number of training areas	Number of Pixels
Arboriculture	21	307
Herbaceous vegetation	13	207
Shrub vegetation	10	290

Continued on next page

Table 1 continued

Irrigated agriculture areas	33	840
Flooded areas	21	294
Rainfed agriculture areas	22	295
Bare soil	3	33
Water bodies	5	65

The image chosen for this study is a Landsat 8 collection 2 tiers 1 TOA image (Path: 197; Row: 53), from 16 March 2019, with less than 10 % cloud cover.

2.5 Classifications assessment

The performance of image classification was assessed using four metrics: the overall accuracy (percentage), the Kappa coefficient of the error matrix,[34–38] the producer accuracy, and the user/consumer accuracy. The Cohen's Kappa coefficient (or Kappa coefficient) is the probability of agreement minus the probability of random agreement, divided by one minus the probability of random agreement; the overall accuracy calculates the total number of correctly classified sites divided by the total number of reference sites[39]; the producer's accuracy is the number of reference pixels classified accurately divided by the total number of reference sites for that class[39]; the producer/user's accuracy is calculating by taking the total number of correct classifications for a particular class and dividing it by the row total[39]. Additionally, a comparison of the areas obtained by classes and by type of classifier was performed to identify convergences between the area values. We compared our results to those obtained by the firm ESRI (Environmental Systems Research Institute) in collaboration with ESA and Microsoft. Indeed, since 2017, ESRI has published a global land cover map every year, using Sentinel-2 images (10 m spatial resolution). The ESRI classification uses the deep learning technique. The accuracies of ESRI maps are between 80 and 90%[40] depending on the type of image used and the number of classes. The classes used by the 2019 ESRI classifications are not exactly identical to our classes; therefore, comparisons were made only for similar classes.

3 Results and Discussion

The five classifications provided good to excellent results based on the assessments of the Kappa coefficients.[34,37] The best Kappa coefficients were obtained by variants of the RF method (Table 2).

Table 2. Evaluation of classification results

Algorithm/Kernel	Overall accuracy (%)	Kappa coefficient
SVM sigmoid function	71.53	0.66
SVM RBF	80.77	0.77
RF 10 forests	93.84	0.92
RF 50 forests	97.69	0.97
RF 100 forests	99.23	0.99

Although the results of all five classifications were good regarding Kappa and overall accuracy values, the detailed performance for each of the classes indicated mixed conclusions (Table 4). The confusion matrices showed lower performance of the SVM classifications compared to those of the RF methods, with accuracies varying between 53.85% to 100% (SVM sigmoid), and 63.64% to 100% (SVM radial basis function). Comparatively, the minimum accuracy found in RF methods was 86.84% (RF 10 forests) (Table 3).

Table 3. Classification accuracies (expressed in %)(*)

	Water	Shrubs	Rainfed	Irrigated	Herbaceous	Flooded	Bare soil	Arboriculture	Prod. Acc.
					Sigmoid				
Water	**70.00**	0	0	0	0	0	0	0	100
Shrubs	0	**76.92**	3.23	0	0	0	0	0	90.91
Rainfed	0	0	**67.74**	3.45	0	0	0	0	95.45
Irrigated	0	15.38	12.90	**68.97**	30	23.08	0	9.52	58.82

Continued on next page

Table 3 continued

Herbaceous	20	0	0	6.90	**60**	23.08	0	0	46.15
Flooded	10	7.69	16.13	13.79	10	**53.85**	0	0	36.84
Bare soil	0	0	0	0	0	0	**100**	0	100
Arboriculture	0	0	0	6.90	0	0	0	**90.48**	90.48
					RBF				
Water	**70.00**	0	0	0	0	0	0	0	100
Shrubs	0	**76.92**	0	3.23	0	0	0	0	90.91
Rainfed	0	0	**88**	0	0	0	0	0	100.00
Irrigated	0	15.38	12	**77.42**	27.27	12.50	0	0	70.59
Herbaceous	20	0	0	3.23	**63.64**	18.75	0	0	53.85
Flooded	10	7.69	0	16.13	9.09	**68.75**	0	0	57.89
Bare soil	0	0	0	0	0	0	**100**	0	100
Arboriculture	0	0	0	0	0	0	0	**100**	100.00
					RF 10				
Water	**100**	0	0	0	0	0	0	0	100
Shrubs	0	**91.67**	0	0	0	0	0	0	100
Rainfed	0	0	**100**	0	0	10	0	0	90.90
Irrigated	0	8.33	0	**86.84**	0	0	0	0	97.05
Herbaceous	0	0	0	5.26	**100**	0	0	0	84.61
Flooded	0	0	0	2.63	0	**90**	0	0	94.73
Bare soil	0	0	0	0	0	0	**100**	0	100
Arboriculture	0	0	0	5.26	0	0	0	**100**	90.47
					RF 50				
Water	**100**	0	0	0	0	0	0	0	100
Shrubs	0	**100**	0	0	0	0	0	0	100
Rainfed	0	0	**95.45**	0	0	5	0	0	95.45
Irrigated	0	0	4.55	**97.06**	0	0	0	0	97.05
Herbaceous	0	0	0	2.94	**100**	0	0	0	92.30
Flooded	0	0	0	0	0	**95**	0	0	100
Bare soil	0	0	0	0	0	0	**100**	0	100
Arboriculture	0	0	0	0	0	0	0	**100**	100
					RF 100				
Water	**100**	0	0	0	0	0	0	0	100
Shrubs	0	**100**	0	0	0	0	0	0	100
Rainfed	0	0	**100**	0	0	5	0	0	95
Irrigated	0	0	0	**100**	0	0	0	0	100
Herbaceous	0	0	0	0	**100**	0	0	0	100
Flooded	0	0	0	0	0	**95**	0	0	100
Bare soil	0	0	0	0	0	0	**100**	0	100
Arboriculture	0	0	0	0	0	0	0	**100**	100

(*) User/consumer accuracy values are shown in the first diagonal of each matrix; Prod. Acc. = Producer accuracy

The spatial distributions of the five classified images are shown in Figure 3. The irrigated agricultural areas were found along the main watercourse (center of each of the images) and northeast of the study area, which corresponds to the sugar cane fields. Water bodies (including that of Lake Tengrela, located at the bottom left of each image) were satisfactorily identified. However, the classification of flooded areas differed between the five classification methods. In SVM classifications, the flooded areas had fairly well-defined contours and were dense. Whereas in RF classifications, these zones seemed to be dispersed, with their contours poorly characterized.

The presence of agricultural areas outside the locations mentioned above is considered erroneous. Indeed, according to the field observations, in March there were few sources of irrigation water apart from the Comoé River. As such, beyond a distance of 1.5 to 2 km on either side of the river, it is unlikely or even impossible for farmers to source their irrigation water from the river. Similarly, the presence of trees in the midst of sugar cane fields is incorrect. The entire sugarcane production area was free of trees, according to the field observations.

SVM algorithms tended to present homogenous classes across the study areas compared to RF algorithms. This tendency was evident in the ESRI Sentinel-2 classification (Figure 4). However, some agricultural areas were falsely identified in the ESRI Sentinel-2 classification. For example, on the right side of the Figure 4, agricultural area outside the sugar company domain

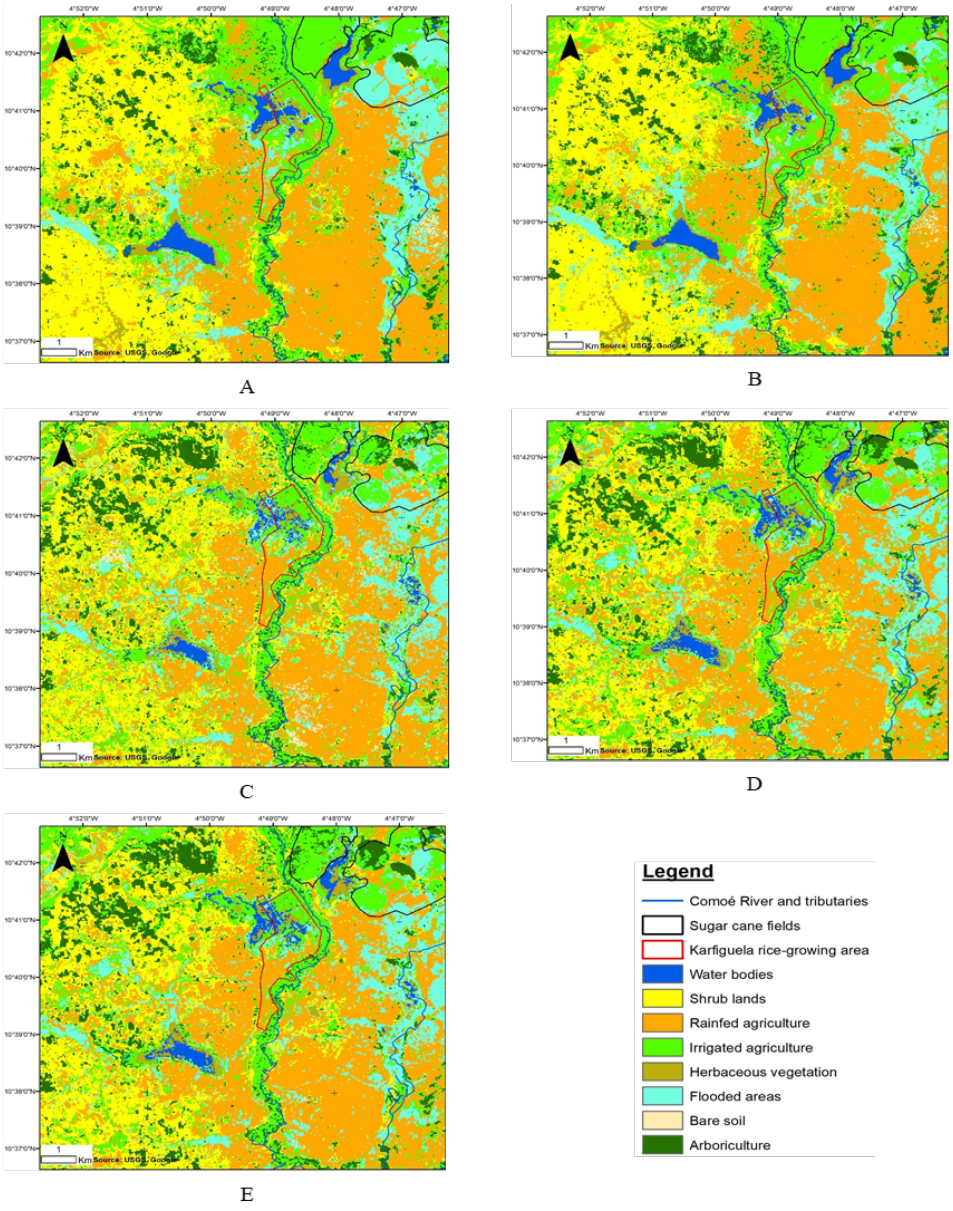

Fig 3. Classifications layout; A: SVM with sigmoid function; B: SVM with RBF function; C: RF with 10 trees; D: RF with 50 trees; E: RF with 100 trees

(located at top right of the Figure) was flooded meadow or vegetation.

A comparison of the surface area values by class for each classifier shows similar results for the majority of the classes, except for the bare soil class (Table 4). This could be explained by the fact that this class is under-represented within the study area. Few pixels were therefore used for training this class, causing disparities between the results of the different classifiers.

Overall, RF methods outperformed SVM in terms of overall accuracy (> 90 %). Indeed, during the evaluation of the results, there was a small percentage of confusion within the classes identified through RF methods. There were recurring confusions between herbaceous vegetation, irrigated vegetation and flooded areas (which maintain hydrophilic vegetation). However, by visually inspecting the maps obtained, the spatial distribution of the classes obtained by the SVM method seems to be close to the reality on the ground.

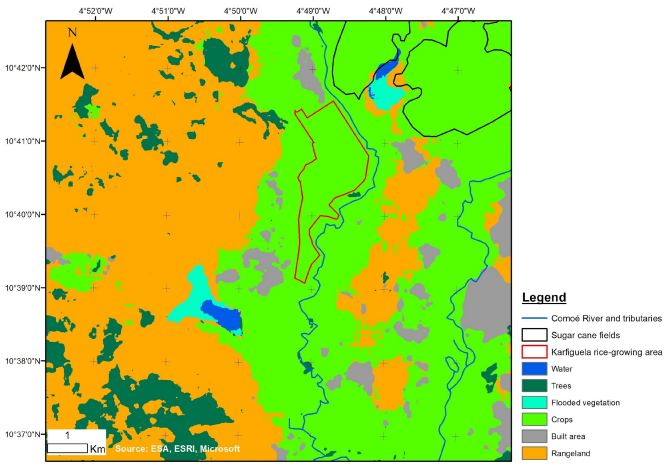

Fig 4. ESRI Sentinel-2 classification of the study area (2019)

Table 4. Estimation of areas by classifier/algorithm and by class

Kernel	Arboricultural	Bare soil	Flooded	Herbaceous	Irrigated	Rainfed	Shrubs	Water
RBF	975.80	28.57	1428.36	373.70	3318.15	4051.23	3840.60	291.42
Sigmoid	823.27	35.16	1422.29	326.58	3195.87	4447.97	3759.02	297.66
RF10	1207.00	144.70	1763.38	375.81	2610.65	4410.08	3605.88	190.32
RF50	1312.58	8.53	1764.79	394.80	2940.49	4659.65	2973.46	253.53
RF100	1385.37	14.94	1679.51	376.08	2864.36	4607.08	3133.63	246.85
Mean	**1140.80**	**46.38**	**1611.67**	**369.40**	**2985.91**	**4435.20**	**3462.52**	**255.96**
Standard dev.	**235.45**	**55.97**	**173.59**	**25.41**	**279.34**	**238.83**	**386.90**	**42.99**
Coeff. Var.	**0.21**	**1.21**	**0.11**	**0.07**	**0.09**	**0.05**	**0.11**	**0.17**

According to Xie[41] and Traoré[13], the success of the supervised classification procedure depends on many factors such as the characteristics of the study area under investigation, the classification system, the remote sensing data and the skills of the analyst. It is therefore difficult to know a priori whether a given classifier will systematically deliver the best results. Numerous comparisons of classifiers exist in the literature,[9,10,42–44] and show that the supremacy of one classifier over another is not always guaranteed, due to application conditions that are not always respected, and quite simply to the difference between the environments to be classified.

4 Conclusion

The study once again demonstrated the potential of remote sensing based approaches for classifying agricultural land areas over large regions and large-scale mapping. The plurality of classification methods/algorithms allow for more flexibility in the choice of the appropriate method according to the data and user experience. The comparison between RF and SVM methods for identifying irrigated land areas across the southern region in Burkina Faso revealed that both methods provided good to excellent classification, with the former outperforming the latter in terms of performance criteria. In terms of spatial distribution of classes, the SVM method provided a mapping close to reality, due to the density of the classes generated. Our results showed that the SVM method was sensitive to class sampling compared to the RF method. Potential research includes the comparison of existing classifiers within the Google Earth Engine environment to classify irrigated areas in Burkina Faso, with the aim of building a near real-time monitoring tool of irrigated land use across the country.

References

1) Palé S, Wellens J, Traoré F, Roncoli C, Sallah AHM, Zangré BVCA, et al. Testing an open app-based water management information system and its uptake among stakeholders in the Upper-Comoé river basin (Burkina Faso). *Water International*. 2021;46(3):417–431. Available from: https:

//doi.org/10.1080/02508060.2021.1897382.
2) Maja MM, Ayano SF. The Impact of Population Growth on Natural Resources and Farmers' Capacity to Adapt to Climate Change in Low-Income Countries. *Earth Systems and Environment*. 2021;5(2):271–283. Available from: https://doi.org/10.1007/s41748-021-00209-6.
3) Zida WA, Traoré F, Bationo BA, Waaub JP. Dynamics of woody plant cover in the Sahelian agroecosystems of the northern region of Burkina Faso since the 1970s–1980s droughts. *Canadian Journal of Forest Research*. 2020;50(7):659–669. Available from: https://doi.org/10.1139/cjfr-2019-0247.
4) Traoré F, Cornet Y, Denis A, Wellens J, Tychon B. Monitoring the evolution of irrigated areas with Landsat images using backward and forward change detection analysis in the Kou watershed, Burkina Faso. *Geocarto International*. 2013;28(8):733–752. Available from: https://doi.org/10.1080/10106049.2012.744100.
5) Enquête Harmonisée sur le Conditions de Vie des Ménages 2018-2019. . Available from: https://doi.org/10.48529/8wh3-bf40.
6) Sawadogo A, Kouadio L, Traoré F, Zwart SJ, Hessels T, Gündoğdu KS. Spatiotemporal Assessment of Irrigation Performance of the Kou Valley Irrigation Scheme in Burkina Faso Using Satellite Remote Sensing-Derived Indicators. *ISPRS International Journal of Geo-Information*. 2020;9(8):1–23. Available from: https://doi.org/10.3390/ijgi9080484.
7) Traoré F, Bonkoungou J, Compaoré J, Kouadio L, Wellens J, Hallot E, et al. Using Multi-Temporal Landsat Images and Support Vector Machine to Assess the Changes in Agricultural Irrigated Areas in the Mogtedo Region, Burkina Faso. *Remote Sensing*. 2019;11(12):1–18. Available from: https://doi.org/10.3390/rs11121442.
8) Sawadogo A, Dossou-Yovo ER, Kouadio L, Zwart SJ, Traoré F, Gündoğdu KS. Assessing the biophysical factors affecting irrigation performance in rice cultivation using remote sensing derived information. *Agricultural Water Management*. 2023;278:1–12. Available from: https://doi.org/10.1016/j.agwat.2022.108124.
9) Zuo W, Mao J, Lu J, Zheng Z, Han Q, Xue R, et al. Mapping Irrigated Areas Based on Remotely Sensed Crop Phenology and Soil Moisture. *Agronomy*. 2023;13(6):1–19. Available from: https://doi.org/10.3390/agronomy13061556.
10) Weitkamp T, Veldwisch GJ, Karimi P, de Fraiture C. Mapping irrigated agriculture in fragmented landscapes of sub-Saharan Africa: An examination of algorithm and composite length effectiveness. *International Journal of Applied Earth Observation and Geoinformation*. 2023;122:1–23. Available from: https://doi.org/10.1016/j.jag.2023.103418.
11) Bastiaanssen WGM, Molden DJ, Makin IW. Remote sensing for irrigated agriculture: examples from research and possible applications. *Agricultural Water Management*. 2000;46(2):137–155. Available from: https://doi.org/10.1016/S0378-3774(00)00080-9.
12) Shinozuka M, Mansouri B. Synthetic aperture radar and remote sensing technologies for structural health monitoring of civil infrastructure systems. *Structural Health Monitoring of Civil Infrastructure Systems*. 2009;p. 113–151. Available from: https://doi.org/10.1533/9781845696825.1.114.
13) Traoré MK. Etude de la couverture et de l'utilisation du sol dans la boucle du Mouhoun : Analyse comparative de 3 classificateurs sur des images satellitaires Landsat 8 et Sentinel 2 . Ouagadougou, Burkina Faso. 2021.
14) Wu Q. GIS and Remote Sensing Applications in Wetland Mapping and Monitoring. *Comprehensive Geographic Information Systems*. 2018;p. 140–157. Available from: https://doi.org/10.1016/B978-0-12-409548-9.10460-9.
15) Li M, Zang S, Zhang B, Li S, Wu C. A Review of Remote Sensing Image Classification Techniques: the Role of Spatio-contextual Information. *European Journal of Remote Sensing*. 2014;47(1):389–411. Available from: https://doi.org/10.5721/EuJRS20144723.
16) Analyse et diagnostic de l'état des lieux des ressources en eau du bassin. Bobo-Dioulasso, Burkina Faso. VREO Project. 2010.
17) Cinquième Recensement Général de la Population et de l'Habitation du Burkina Faso : Synthèse des résultats définitifs. Ouagadougou, Burkina Faso. INSD. 2022. Available from: http://cns.bf/IMG/pdf/plaquette_resultats_definitifs_rgph_2019_-_revu_30-12-2022.pdf.
18) Palé S, Traoré F, Wellens J, Tychon B. Diagnostic d'un système d'informations de gestion de l'eau à usage agricole dans le sous-bassin versant de la Haute-Comoé. *Geo-Eco-Trop*. 2019;43(3):433–443. Available from: https://www.geoecotrop.be/uploads/publications/pub_433_13.pdf.
19) Rodriguez-Galiano VF, Ghimire B, Rogan J, Chica-Olmo M, Rigol-Sanchez JP. An assessment of the effectiveness of a random forest classifier for land-cover classification. *ISPRS Journal of Photogrammetry and Remote Sensing*. 2012;67:93–104. Available from: https://doi.org/10.1016/j.isprsjprs.2011.11.002.
20) Ustuner M, Sanli FB, Dixon B. Application of Support Vector Machines for Landuse Classification Using High-Resolution RapidEye Images: A Sensitivity Analysis. *European Journal of Remote Sensing*. 2015;48(1):403–422. Available from: https://doi.org/10.5721/EuJRS20154823.
21) Mountrakis G, Im J, Ogole C. Support vector machines in remote sensing: A review. *ISPRS Journal of Photogrammetry and Remote Sensing*. 2011;66(3):247–259. Available from: https://doi.org/10.1016/j.isprsjprs.2010.11.001.
22) Vapnik VN. The Nature of Statistical Learning Theory. 2nd ed. Information Science and Statistics;New York, NY, USA. Springer. 2000. Available from: https://doi.org/10.1007/978-1-4757-3264-1.
23) Anthony G, Greg H, Tshilidzi M. Classification of Images Using Support Vector Machines . . Available from: https://arxiv.org/ftp/arxiv/papers/0709/0709.3967.pdf.
24) Hsu CW, Chang CC, Lin CJ. A Practical Guide to Support Vector Classification. Taipei, Taiwan. National Taiwan University. 2003. Available from: https://www.csie.ntu.edu.tw/~cjlin/papers/guide/guide.pdf.
25) Foody GM, Mathur A. A relative evaluation of multiclass image classification by support vector machines. *IEEE Transactions on Geoscience and Remote Sensing*. 2004;42(6):1335–1343. Available from: https://doi.org/10.1109/TGRS.2004.827257.
26) Wu TF, Lin CJ, Weng RC. Probability Estimates for Multi-class Classification by Pairwise Coupling. *Journal of Machine Learning Research*. 2004;5:975–1005. Available from: https://www.csie.ntu.edu.tw/~cjlin/papers/svmprob/svmprob.pdf.
27) Breiman L. Random Forests. *Machine Learning*. 2001;45(1):5–32. Available from: https://doi.org/10.1023/A:1010933404324.
28) Tumer K, Ghosh J. Analysis of decision boundaries in linearly combined neural classifiers. *Pattern Recognition*. 1996;29(2):341–348. Available from: https://doi.org/10.1016/0031-3203(95)00085-2.
29) Inglada J, Vincent A, Arias M, Tardy B, Morin D, Rodes I. Operational High Resolution Land Cover Map Production at the Country Scale Using Satellite Image Time Series. *Remote Sensing*. 2017;9(1):1–35. Available from: https://doi.org/10.3390/rs9010095.
30) Gislason PO, Benediktsson JA, Sveinsson JR. Random Forests for land cover classification. *Pattern Recognition Letters*. 2006;27(4):294–300. Available from: https://doi.org/10.1016/j.patrec.2005.08.011.
31) Pal M. Random forest classifier for remote sensing classification. *International Journal of Remote Sensing*. 2005;26(1):217–222. Available from: https://doi.org/10.1080/01431160412331269698.
32) Belgiu M, Drăguţ L. Random forest in remote sensing: A review of applications and future directions. *ISPRS Journal of Photogrammetry and Remote Sensing*. 2016;114:24–31. Available from: https://doi.org/10.1016/j.isprsjprs.2016.01.011.
33) Lassalle P, Inglada J, Michel J, Grizonnet M, Malik J. A Scalable Tile-Based Framework for Region-Merging Segmentation. *IEEE Transactions on Geoscience and Remote Sensing*. 2015;53(10):5473–5485. Available from: https://doi.org/10.1109/TGRS.2015.2422848.

34) Landis JR, Koch GG. The Measurement of Observer Agreement for Categorical Data. *Biometrics*. 1977;33(1):159–174. Available from: https://doi.org/10.2307/2529310.
35) Banko G. A Review of Assessing the Accuracy of Classifications of Remotely Sensed Data and of Methods Including Remote Sensing Data in Forest Inventory. 1998. Available from: https://core.ac.uk/reader/33897040.
36) Foody GM. Status of land cover classification accuracy assessment. *Remote Sensing of Environment*. 2002;80(1):185–201. Available from: https://doi.org/10.1016/S0034-4257(01)00295-4.
37) Streiner DL, Norman GR, Cairney J. Health Measurement Scales: A Practical Guide to Their Development and Use. 5th ed. USA. Oxford University Press. 2014. Available from: https://doi.org/10.1093/med/9780199685219.001.0001.
38) Congalton RG, Green K. Assessing the Accuracy of Remotely Sensed Data: Principles and Practices. 2nd ed. Boca Raton. CRC Press. 2008. Available from: https://doi.org/10.1201/9781420055139.
39) Accuracy Metrics. 2019. Available from: https://gsp.humboldt.edu/olm/Courses/GSP_216/lessons/accuracy/metrics.html.
40) Land Cover Classification (Sentinel-2). 2023. Available from: https://www.arcgis.com/home/item.html?id=afd124844ba84da69c2c533d4af10a58.
41) Xie Z, Chen Y, Lu D, Li G, Chen E. Classification of Land Cover, Forest, and Tree Species Classes with ZiYuan-3 Multispectral and Stereo Data. *Remote Sensing*. 2019;11(2):1–27. Available from: https://doi.org/10.3390/rs11020164.
42) Avci C, Budak M, Yağmur N, Balçik FB. Comparison between random forest and support vector machine algorithms for LULC classification. *International Journal of Engineering and Geosciences*. 2023;8(1):1–10. Available from: https://dergipark.org.tr/en/download/article-file/1943956.
43) Adugna T, Xu W, Fan J. Comparison of Random Forest and Support Vector Machine Classifiers for Regional Land Cover Mapping Using Coarse Resolution FY-3C Images. *Remote Sensing*. 2022;14(3):1–22. Available from: https://doi.org/10.3390/rs14030574.
44) Sabat-Tomala A, Raczko E, Zagajewski B. Comparison of Support Vector Machine and Random Forest Algorithms for Invasive and Expansive Species Classification Using Airborne Hyperspectral Data. *Remote Sensing*. 2020;12(3):1–21. Available from: https://doi.org/10.3390/rs12030516.